Synthesis of an η^2-N_2-Titanium Diazoalkane Complex with Both Imido- and Metal Carbene-Like Reactivity Patterns

Jennifer L. Polse, Anne W. Kaplan, Richard A. Andersen,* and Robert G. Bergman*

Contribution from the Department of Chemistry, University of California, Berkeley, California 94720

Received December 19, 1997

Abstract: The novel η^2-N_2-diazoalkane complex $Cp^*_2Ti(N_2CHSiMe_3)$ (**2**) has been prepared by addition of (trimethylsilyl)diazomethane to $Cp^*_2Ti(C_2H_4)$ (**1**). The structure of **2** reveals nearly symmetric Ti−N distances and an N−N distance ∼0.1 Å longer than that of the free diazoalkane. Compound **2** loses dinitrogen in solution under mild conditions to give the fulvene complex $Cp^*FvTiCH_2SiMe_3$ (**4**). Thermolysis of **2** in the presence of 1-alkenes yields the trans-α,β-disubstituted titanacyclobutane complexes $Cp^*_2Ti(CH(SiMe_3)CH(R)CH_2)$ (R = H (**6**), R = Ph (**7**), R = Me (**8**), R = Et (**9**)). The regio- and stereochemistry of the titanacyclobutane complexes was determined by a combination of one- and two-dimensional NMR techniques. The NMR assignment was supported in the case of **8** by an X-ray diffraction study. In addition to confirming the regio- and stereochemistry of the metallacycle, the X-ray structure of **8** shows that unlike most titanacyclobutanes, the metallacycle ring is puckered. A kinetic study of the formation of **7** from **2** and styrene revealed that the reaction is first order in **2** and zero order in styrene. The rate constant for this reaction is identical to that measured for the conversion of **2** to **4**. The kinetic study supports a mechanism involving initial rate-determining loss of dinitrogen to form a carbene complex intermediate which undergoes hydrogen transfer from a Cp* methyl to give **4**, or in the presence of styrene is trapped to form **7**. In addition to its metal carbene-like reactions involving N_2 loss, complex **2** undergoes a variety of transformations in which N_2 is retained in the final product. These include cycloaddition reactions with alkynes and allene, as well as reversible reactions with Lewis bases to form adducts. These transformations, which are similar to reactions of group IV imido complexes, demonstrate the imide-like character of the diazoalkane ligand.

Introduction

Diazoalkanes have long been used as synthons for both free carbenes and metal carbene complexes (eq 1).[1−4] In the metal

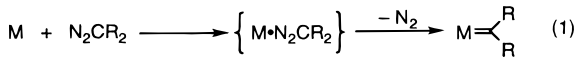

(1)

carbene syntheses, it is generally assumed that an intermediate diazoalkane complex is involved in the carbene-transfer process. Diazoalkane complexes have also been implicated as intermediates in the metal-catalyzed cyclopropanation of olefins by diazoalkanes (eq 2).[2,5−7]

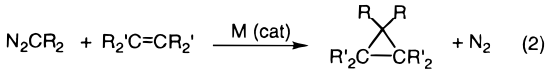

(2)

An understanding of the reactivity of diazoalkane complexes would aid in further development of such catalysts. Unfortunately, while there are numerous examples of transition metal diazoalkane complexes, they are typically quite resistant to N_2 loss.[3,4] As a result, few isolable diazoalkane complexes have been shown to generate metal carbene complexes.[8−12] We recently reported a novel titanocene diazoalkane complex that undergoes facile N_2 loss.[13] This complex also undergoes a variety of reactions that proceed with retention of N_2, including cycloaddition reactions with alkynes and allene that are strikingly similar to those of group IV imido complexes. This paper reports the full details of the synthesis of the diazoalkane complex and of its carbene- and imido-like reactivity patterns.

Results

Synthesis and Characterization of $Cp^*_2Ti(N_2CHSiMe_3)$ (2). Treatment of a toluene or benzene solution of $Cp^*_2Ti(C_2H_4)$ (**1**) with 1 equiv of (trimethylsilyl)diazomethane results in gas evolution and an immediate color change from lime to forest green. Use of exactly equimolar amounts of the two reactants is critical to the clean isolation of the product $Cp^*_2Ti(N_2CHSiMe_3)$ (**2**), because it decomposes in the presence of excess diazoalkane. Removal of the solvent gives a green powder that may be crystallized from hexanes at −50 °C to give pure **2** in 60−70% yield (eq 3).

(1) For a very recent example, see: Schwab, P.; Grubbs, R. H.; Ziller, J. W. *J. Am. Chem. Soc.* **1996**, *118*, 100.
(2) Mizobe, Y.; Ishii, Y.; Hidai, M. *Coord. Chem. Rev.* **1995**, *139*, 281.
(3) Herrmann, W. A. *Angew. Chem., Int. Ed. Engl.* **1978**, *17*, 800.
(4) Sutton, D. *Chem. Rev.* **1993**, *93*, 995.
(5) Herrmann, W. A.; Menjon, B.; Herdtweck, E. *Organometallics* **1991**, *10*, 2134.
(6) Doyle, M. P.; Peterson, L. S.; Zhou, Q. L.; Nishiyama, H. *Chem. Commun.* **1997**, 211.
(7) Doyle, M. P.; Peterson, C. S.; Parker, D. L., Jr. *Angew. Chem., Int. Ed. Engl.* **1996**, *35*, 1334.
(8) Messerle, L.; Curtis, M. D. *J. Am. Chem. Soc.* **1980**, *102*, 7789.
(9) Curtis, M. D.; Messerle, L.; D′Errico, J. J.; Butler, W. M.; Hay, M. S. *Organometallics* **1986**, *5*, 2283.
(10) Nakamura, A.; Yoshida, T.; Cowie, M.; Otsuka, S.; Ibers, J. A. *J. Am. Chem. Soc.* **1977**, *99*, 2108.
(11) Cowie, M.; Loeb, S. J.; McKeer, I. R. *Organometallics* **1986**, *5*, 854.
(12) Clauss, A. D.; Shapley, J. R.; Wilson, S. R. *J. Am. Chem. Soc.* **1981**, *103*, 7387.
(13) Polse, J. L.; Andersen, R. A.; Bergman, R. G. *J. Am. Chem. Soc.* **1996**, *118*, 8737.

S0002-7863(97)04303-5 CCC: $15.00
Published on Web 06/12/1998

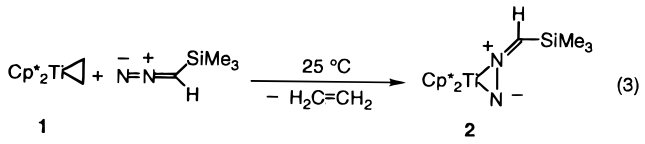

(3)

The modest isolated yield reflects the high solubility of the complex rather than the formation of any byproducts. When the reaction is performed in benzene-d_6 and followed by ^{1}H NMR spectroscopy, 1 equiv of free ethylene is produced in addition to **2** in >98% yield, which is the only observable titanium-containing product. Retention of the nitrogen atoms in **2** was confirmed by mass spectroscopy, elemental analysis, and X-ray crystallography (vide infra).

The ^{1}H NMR spectrum of **2** displays singlets at 0.44 and 1.71 ppm for the Me_3Si and equivalent Cp* groups, respectively. In addition, there is a singlet at 4.11 ppm that is assigned to the methine proton of the diazoalkane ligand. The $^{13}C\{^1H\}$ NMR spectrum, in addition to resonances for the Cp* and Me_3Si groups, shows a methine resonance at 99.9 ppm for the diazoalkane ligand. The IR spectrum does not contain any strong absorptions in the region typically associated with organic diazoalkanes (2000−2270 cm^{-1}). The lack of a strong infrared stretch in this region for the diazoalkane ligand probably results from reduction of the N−N bond order due to back-bonding from the metal center (vide infra).[14]

Because of the wide variety of possible coordination modes for diazoalkane ligands, it is often difficult to predict their structures based on spectroscopic data. We therefore undertook a single-crystal X-ray diffraction study to determine the coordination mode of the diazoalkane ligand in **2**. The structure was solved by direct methods and refined using standard least-squares and Fourier techniques. Crystal data and collection parameters are given in Table 1. An ORTEP diagram is shown in Figure 1, and representative bond lengths and angles are given in Table 2. Other details of the structure determination are provided in the Experimental Section and as Supporting Information. The structural study reveals that the diazoalkane ligand is bound to the titanium in a side-on fashion through the two nitrogen atoms. Although side-on coordination is less common than end-on or bridging coordination modes, it is not unprecedented.[2−4,10,15,16] As is usually the case for side-bound diazoalkane complexes,[4] the Ti−N1 (1.979(2) Å) and Ti−N2 (2.012(2) Å) distances for **2** are very similar. The Ti−N2 distance is slightly longer than the Ti−N1 distance, possibly because N1 is two-coordinate and therefore has a smaller radius than does N2.[17] The Ti−N distances are indicative of single bonds, and are similar to the Ti−N1 distance (1.980(5) Å) in the diazoalkane complex Cp_2Ti(DEDM) (DEDM = diethyldiazomalonate) (**3**) (Scheme 1) synthesized by Floriani.[15] The other Ti−N distance in **3** is quite long (2.219(7) Å), possibly because of a large contribution from resonance structure **B** (Scheme 1).

The bonding situation in **2** is similar to that in an olefin adduct. The relatively long N−N bond distance (1.276(3) Å) compared with that of uncomplexed diazoalkanes (1.12−1.13 Å)[18] indicates substantial π-back-bonding from the b_2 orbital of the titanocene fragment to the diazoalkane LUMO, which is N−N antibonding.[19] The N−N distance is indicative of a partial N−N double bond, since N−N single bonds are typically ~1.40

Table 1. Crystal Data for **2**, **8**, and **18**

	2	**8**	**18**
diffractometer	Siemens Smart	Siemens Smart	Siemens Smart
T (°C)	−99.0	−100.0	−109.0
radiation	Mo Kα (λ = 0.71069 Å)	Mo Kα (λ = 0.71069 Å)	Mo Kα (λ = 0.71069 Å)
take-off angle (deg)	6.0	6.0	6.0
cryst-to-detec dist (mm)	60	60	60
scan type	ω(0.3°/frame)	ω(0.3°/frame)	ω(0.3°/frame)
scan rate (s/frame)	30.0	10.0	10.0
$2\theta_{max}$ (deg)	46.5	51.6	51.9
no. of refl. collected	9838	12217	7493
no. of unique refl.	3629	4740	4601
no. of obsd reflns $I > 3.00\sigma(I)$	2904	2809	3941
no. of variables	414	400	280
refl/parameter ratio	7.01	7.02	14.07
R	0.045	0.043	0.039
R_w	0.058	0.050	0.057
goodness of fit	2.23	1.68	2.15
p factor	0.01	0.01	0.03

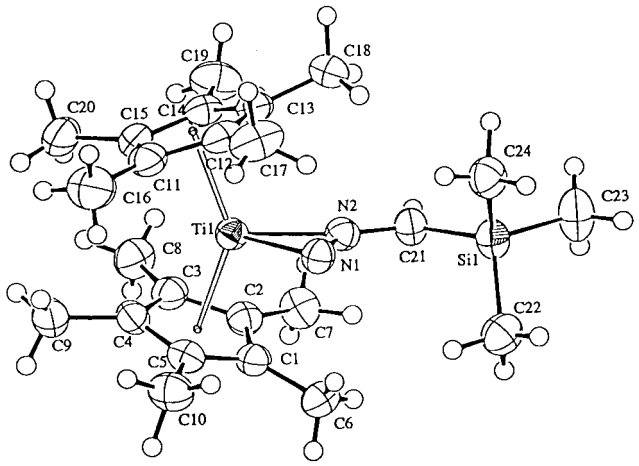

Figure 1. ORTEP diagram of $Cp^*_2Ti(N_2CHSiMe_3)$ (**2**).

Table 2. Selected Bond Distances (Å) and Angles (deg) for **2**

Ti−N1	1.979(2)	Ti−N2	2.012(2)
Ti−Cp*1	2.0961(4)	Ti−Cp*2	2.0970(4)
N1−N2	1.276(3)	N2−C21	1.342(3)
Si1−C21	1.840(3)		
Cp*1-Ti−Cp*2	140.72(2)	N1−Ti−Cp*1	109.05(6)
N1−Ti−Cp*2	108.51(6)	N2−Ti−Cp*1	106.68(6)
N2−Ti−Cp*2	110.03(6)	N1−Ti−N2	37.27(9)
Ti−N2−C21	158.7(2)	N1−N2−C21	131.3(2)
Si1−C21−N2	122.6(2)	Ti−N1−N2	72.8(1)

Scheme 1

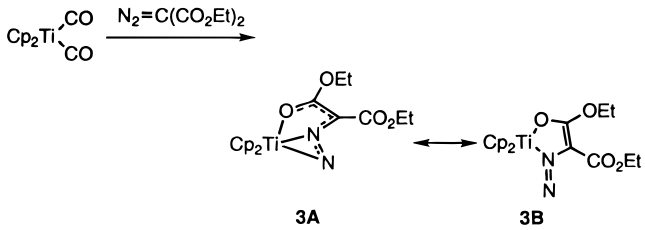

(14) The IR spectrum of **2** contains a weak stretch at 1894 cm^{-1} which may be due to a reduced N−N bond stretch; however, it has not been assigned.

(15) Gambarotta, S.; Floriani, C.; Chiesi-Villa, A.; Guastini, C. *J. Am. Chem. Soc.* **1982**, *104*, 1918.

(16) Schramm, K. D.; Ibers, J. A. *Inorg. Chem.* **1980**, *19*, 2441.

(17) Pauling, L. *The Nature of the Chemical Bond*; Cornell University Press: Ithaca, New York, 1967.

(18) Patai, S. *The Chemistry of Diazonium and Diazo Groups, Parts 1 and 2*; Wiley: New York, 1978 and references therein.

(19) Jorgensen, W. L.; Salem, L. *The Organic Chemist's Book of Orbitals*; Academic Press: New York, 1973; p 126.

Scheme 2

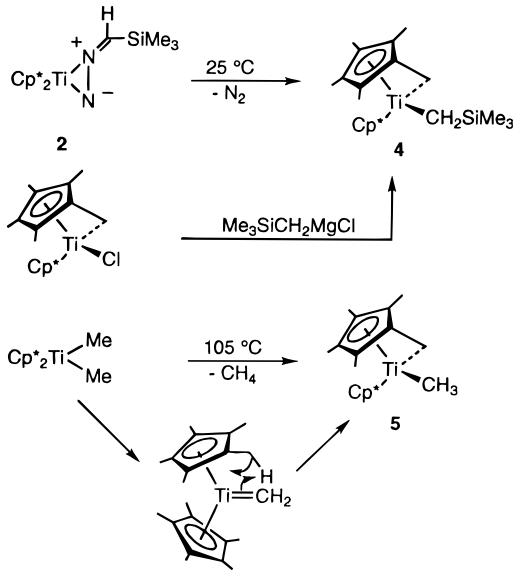

Å.[20] In this respect, the structure of **2** is similar to that of the starting olefin complex **1**. Compound **1** has a C−C bond length of 1.438 (5) Å for the ethylene ligand, which is ∼0.1 Å longer than its value in free ethylene, indicating that complex **1** is best described as intermediate between a titanium(II) olefin adduct and a titanium(IV) metallacyclopropane.[21]

Thermal N_2 Loss and Formation of Cp*FvTiCH$_2$SiMe$_3$ (Fv = η^5,η^1-Me$_4$C$_5$CH$_2$) (4). Complex **2** is thermally unstable in both the solid and solution states. It decomposes at 25 °C in the solid state with a half-life of ∼20 h to give a red powder. This powder has not been identified, but on the basis of its low solubility it is presumed to be polymeric in nature. In benzene and toluene solution **2** decomposes with a half-life of 2 h at 32 °C to give fulvene complex **4** in 84% isolated yield (Scheme 2). Complex **4** was identified on the basis of its NMR spectral data and elemental analysis. In addition, **4** was independently synthesized as described previously.[13,22] The inequivalent methyl groups of the metalated Cp* ring are clearly visible in both the ^{1}H and ^{13}C{^{1}H} NMR spectra of **4**. The protons on both methylene carbons are diastereotopic, and therefore the ^{1}H NMR spectrum shows two sets of doublets for these protons. The resonances due to the methylene protons of the trimethylsilylmethyl ligand show silicon satellites, and they can therefore be distinguished from the two doublets of the fulvene methylene group. A ^{1}H−^{13}C HMQC[23] spectrum showed that the Me_3SiCH_2 methylene protons correlate with the methylene resonance at 45.8 in the ^{13}C{^{1}H} NMR spectrum. The methylene carbon of the fulvene ligand resonates at 76.1 ppm in the ^{13}C{^{1}H} NMR spectrum. This is well within the typical range observed for titanium fulvene complexes. For example, the CH_2 group of Cp*FvTiCH$_3$ (**5**), prepared earlier from Cp*$_2$TiMe$_2$ (Scheme 2), resonates at 73.9 ppm in the ^{13}C{^{1}H} NMR spectrum.[24]

Reactivity of 2 toward Terminal Alkenes. Formation of Metallacyclobutane Complexes. Compound **2** reacts with terminal alkenes H_2C=CHR (R = H, Ph, Me, Et) over a period of 2 d at room temperature to give the deep red metallacyclobutane complexes **6**−**9** (Scheme 3) in good yield. Loss of dinitrogen was confirmed by elemental analysis. The ^{1}H NMR spectra of these materials show the expected features, including inequivalent Cp* ligands. In the case of substituted olefins, there are six distinct metallacycle isomers that may be formed (Figure 2). We observe that alkene addition to **2** is regio- and stereospecific, since we observe only one of these possible isomers. This isomer was identified as α,*β*-disubstituted isomer **A** (Figure 2) by a combination of one- and two-dimensional NMR techniques as described below. 1-Butene was the most sterically hindered alkene that still gave complete conversion to the metallacycle product; reaction of **2** with the bulkier olefin 3-methylbutene gave a mixture of fulvene complex **4** and the expected metallacyclobutane. Thermolysis of **2** in the presence of even bulkier α-olefins such as 3,3-dimethylbutene gave exclusively **4**. Complex **2** does not react with internal olefins or alkynes including the strained cyclic olefin norbornadiene.

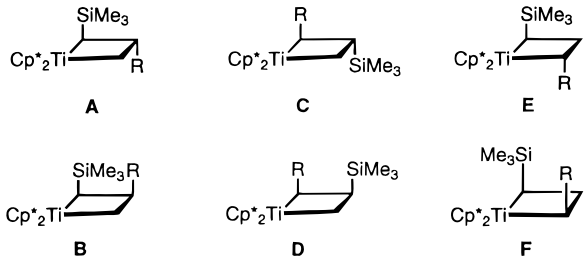

Figure 2. Isomers of disubstituted metallacyclobutanes.

Scheme 3

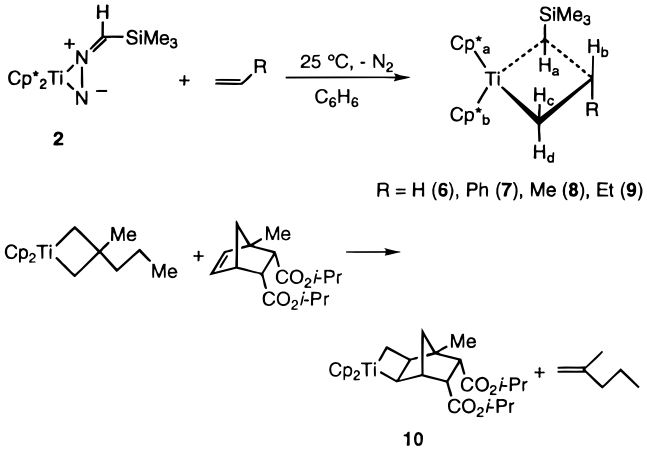

NMR Determination of the Regio- and Stereochemistry of Metallacyclobutane Complexes 6−9. The regiochemistry of the metallacyclobutane complexes was determined as follows. The ^{1}H NMR spectra of **7**−**9** (Scheme 3) display several distinguishing features, including diastereotopic Cp* resonances, a trimethylsilyl group, and several strongly coupled resonances between −0.9 and 2 ppm for the protons in the metallacycle ring. In addition to peaks for the Cp* ligands and trimethylsilyl groups, the ^{13}C{^{1}H} NMR spectra of **7**−**9** show two resonances between 60 and 70 ppm, which is within the region associated with α-carbons of titanacyclobutanes.[25−30] By using standard

(20) Allen, F. H.; Kennard, O.; Watson, D. G.; Brammer, L.; Orpen, A. G.; Taylor, R. *J. Chem. Soc., Perkin Trans.* **1987**, S1.
(21) Cohen, S. A.; Auburn, P. R.; Bercaw, J. E. *J. Am. Chem. Soc.* **1983**, *105*, 1136.
(22) Luinstra, G. A.; Brinkmann, P. H. P.; Teuben, J. H. *J. Organomet. Chem.* **1997**, *532*, 125.
(23) Bax, A.; Subramanian, S. *J. Magn. Reson.* **1986**, *67*, 565.
(24) McDade, C.; Green, J. C.; Bercaw, J. E. *Organometallics* **1982**, *1*, 1629.
(25) Lee, J. B.; Gajda, G. J.; Schaefer, W. P.; Howard, T. R.; Ikariya, T.; Straus, D. A.; Grubbs, R. H. *J. Am. Chem. Soc.* **1981**, *103*, 7358.
(26) Lee, J. B.; Ott, K. C.; Grubbs, R. H. *J. Am. Chem. Soc.* **1982**, *104*, 7491.
(27) Howard, T. R.; Lee, J. B.; Grubbs, R. H. *J. Am. Chem. Soc.* **1980**, *102*, 6876.
(28) Gilliom, L. R.; Grubbs, R. H. *Organometallics* **1986**, *5*, 721.
(29) Straus, D. A.; Grubbs, R. H. *J. Mol. Catal.* **1985**, *28*, 9.

DEPT pulse sequences, these resonances were determined to arise from one methine and one methylene carbon, indicating that the metallacycles are α,β-disubstituted. (This restricts the possible structures to isomers **A**−**D** in Figure 2.) The ^{1}H NMR spectra of **7**−**9** each display a doublet integrating to one proton between 1.2 and 2 ppm. This proton signal correlates with the downfield methine resonance in a one-bond ^{1}H−^{13}C HMQC NMR experiment.[23] In several cases, silicon satellites were observed for this methine resonance in the ^{1}H NMR spectrum, indicating that the trimethylsilyl group is directly bonded to the methine carbon. The metallacycle methines not bound to titanium resonated between 15 and 30 ppm in the ^{13}C{^{1}H} NMR spectrum. The ^{1}H−^{1}H COSY NMR spectra of **8** and **9** revealed that the proton resonance that correlated with the central methine carbon was strongly coupled to the protons of the methyl or ethyl substituent. None of the other metallacyclobutane ring protons were coupled to the methyl or ethyl substituents. Taken together, these data indicate that the trimethylsilyl-substituted carbon resonance is α to the metal center, limiting the choices to isomers **A** and **B** in Figure 2.

To determine the relative stereochemistry of the metallacycle methine carbons in **7**−**9** (i.e., to distinguish between isomers **A** and **B**), ^{1}H−^{1}H NOESY spectra were acquired as described in the Experimental Section. The analysis was similar for each metallacycle and will be described in detail for the 1-butene adduct **9**. The NOESY spectrum of **9**, acquired using a mixing time of 792 ms, is given as Supporting Information. The substituent labeling used in the following discussion is shown in Scheme 3. Cross-peaks were observed between Cp^*_a and the Me_3Si group, H_b and H_c. Cp^*_b showed NOE's to H_d, the ethyl group, and H_a. No NOE's were observed between the ring protons and the Cp* on the opposite side of the ring from them. If the substituents were in a cis arrangement (isomer **B**, Figure 2), the two ring methine resonances (H_a and H_b) would be expected to show cross-peaks to the same Cp*. Instead, each shows a cross-peak to a different Cp*. Only the trans isomer is consistent with the observed pattern of cross-peaks. Together with the HMQC and COSY NMR data, the NOESY experiments indicate that the disubstituted metallacyclobutanes possess structure **A** (Figure 2).

Only two isomers are possible for metallacycle **6**, since in this case isomers **C**−**F** are all equivalent, and **A** and **B** are equivalent (Figure 2). The two possible isomers have the trimethylsilyl group α or β to the metal center. In addition to the expected trimethylsilyl and diastereotopic Cp* resonances, the ^{13}C{^{1}H} NMR spectrum of **6** shows two resonances, at 71.1 and 73.2 ppm. Using standard DEPT pulse sequences, these resonances were assigned to methylene and methine carbons, respectively. As discussed above, these resonances are due to the α carbons of the metallacyclobutane ring. This indicates that, as in **7**−**9**, the trimethylsilyl-substituted carbon is α to the metal center in **6**.

X-ray Structure of $Cp^*_2Ti(CH(SiMe_3)CH(Me)CH_2)$ (8). To confirm the NMR assignment of the structures of **6**−**9**, a single-crystal X-ray diffraction study of propene adduct **8** was undertaken. The structure was solved by Patterson methods and refined using standard least squares and Fourier techniques. Crystal and data collection parameters are shown in Table 1, and details of the structure determination are given in the Experimental Section. Positional and thermal parameters are given in Tables S7 and S8 of the Supporting Information. An ORTEP diagram of **8** is shown in Figure 3. Table 3 provides intramolecular bond lengths and angles for this compound. As expected from the NMR experiments, the two substituents are on adjacent carbons and are trans to one another. The structure also shows that the trimethylsilyl-substituted carbon is α to the metal center. The Ti−C21 and Ti−C23 distances are statistically different (2.155(4) and 2.192(4) Å, respectively) but essentially equivalent and are within the typical range (2.14−2.21 Å) for Ti−C_{sp^3} bonds.[31] The C−C distances in the metallacycle ring are similar to those of previously characterized titanacyclobutane complexes.[25] The ring is puckered with a dihedral angle of 28° between the C21TiC23 and C21C22C23 planes. Although the vast majority of structurally characterized titanacyclobutanes are planar, puckering of the ring has been observed previously in an α,β-disubstituted titanacyclobutane **10** (Scheme 3) derived from Tebbe's reagent and a norbornene diester.[30] The distortion in the case of **8** is probably a result of the extreme steric congestion between the metal center and the two ring substituents.

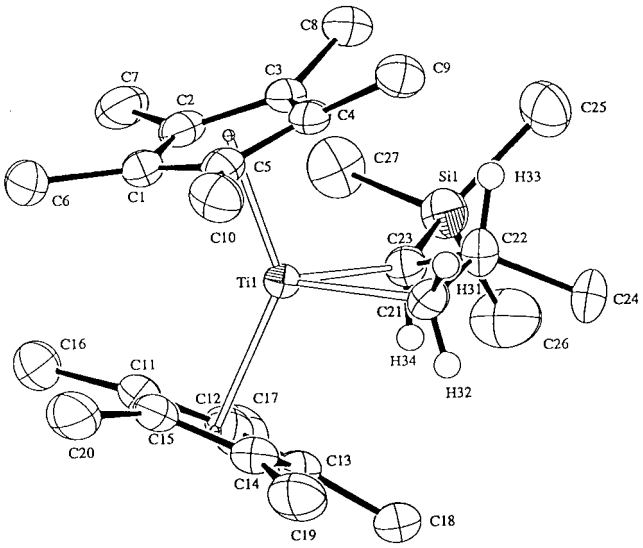

Figure 3. ORTEP diagram of $Cp^*_2Ti(CH(SiMe_3)CH(Me)CH_2)$ (**8**).

Table 3. Selected Bond Distances (Å) and Angles (deg) for **8**

Ti−C21	2.155(4)	Ti−C23	2.192(4)
Ti−Cp*1	2.1447(6)	Ti−Cp*2	2.1600(6)
C21−C22	1.551(5)	C22−C23	1.557(5)
Si1−C23	1.873(4)	C22−C24	1.533(5)
Cp*1−Ti−Cp*2	135.78(3)	C21−Ti−Cp*1	104.7(1)
C21−Ti−Cp*2	106.4(1)	C23−Ti−Cp*1	111.4(1)
C23−Ti−Cp*2	108.0(1)	C21−Ti−C23	71.2(1)
Ti−C21−C22	87.6(2)	Ti−C23−C22	86.1(2)
C21−C22−C23	109.0(3)	Ti−C23−Si1	145.9(2)
C23−C22−C24	113.5(3)	C21−C22−C24	111.5(3)

To determine whether the observed isomer is the kinetic rather than the thermodynamic product of the reaction of **2** with alkenes a solution of styrene adduct **7** in C_6D_6 was heated to 45 °C for 2 d. No rearrangement of **7** was observed. However, heating to 75 °C resulted in formation of fulvene complex **4**. This is likely the result of a retrocyclization of the metallacycle to form a transient carbene complex which then reacts with a C−H bond of the ligand (vide infra). Attempts to exchange one alkene for another in the metallacyclobutanes were unsuccessful. For instance, heating the 1-butene adduct **9** to 75 °C in the presence of 8 equiv of styrene resulted only in formation of **4** and release of butene. The released butene was a mixture

(30) Stille, J. R.; Santarsiero, B. D.; Grubbs, R. H. *J. Org. Chem.* **1990**, *55*, 843.

(31) Orpen, A. G.; Brammer, L.; Allen, F. H.; Kennard, O.; Watson, D. G.; Taylor, R. *J. Chem. Soc., Dalton Trans.* **1989**, S1.

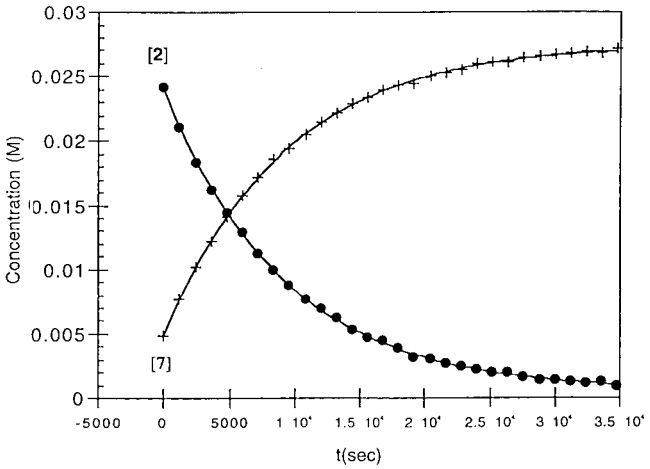

Figure 4. Plot of concentration vs time and exponential fit for the formation of **7** from **2** and styrene at 32 °C.

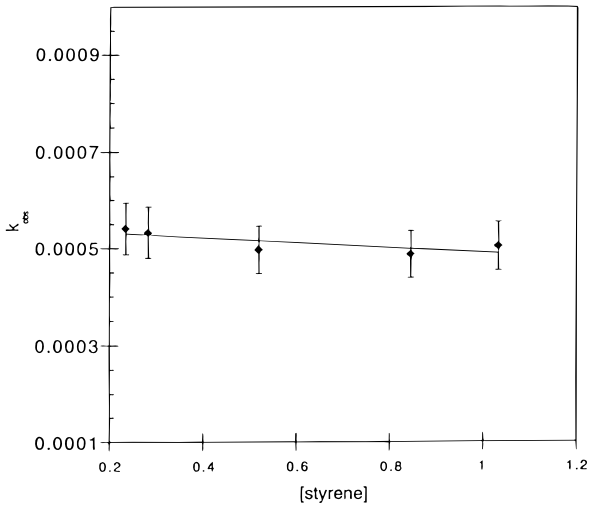

Figure 5. Plot of k_{obs} vs styrene concentration for the reaction of **2** with styrene.

of *cis*- and *trans*-2-butene, rather than the expected 1-butene; the mechanism of isomerization of the butene is unknown at this time.

Kinetic Study of Formation of 7 from 2 and Styrene. The kinetics of the reaction of diazoalkane complex **2** with styrene in toluene-d_8 have been examined by ^{1}H NMR spectroscopy at a variety of temperatures and styrene concentrations. To ensure that the reaction would be pseudo-first-order in **2**, the lowest styrene concentration examined was 10 times greater than the concentration of **2**. A typical plot of concentration vs time is shown in Figure 4. The reaction follows first-order kinetics to >5 half-lives. A plot of k_{obs} vs [styrene] (Figure 5) demonstrates that the reaction rate is independent of styrene concentration. An Eyring plot (30−60 °C) (Figure 6) gives $\Delta H^{\ddagger} = 22.5 \pm 0.3$ kcal/mol, $\Delta S^{\ddagger} = -3.1 \pm 1.0$ eu, and $\Delta G^{\ddagger} = 23.4 \pm 0.4$ kcal/mol (calculated at 25 °C). To assess whether any charge buildup occurs in the transition state, the rate of the reaction was also measured at 45.7 °C in the more polar solvent, THF-d_8. The rate constant was 6.04×10^{-4} ($\pm$ 0.01×10^{-4}) s^{-1}, which is the same within error as that measured in toluene-d_8 at the same temperature. At 45 °C in toluene-d_8, **2** rearranges to fulvene complex **4** with a k_{obs} of 5.17×10^{-4} ($\pm$ 0.10×10^{-4}) s^{-1}, identical within experimental error to that for the reaction of **2** with styrene at 45 °C of 5.02×10^{-4} ($\pm$ 0.04×10^{-4}) s^{-1}. The formation of the fulvene complex **4** from **2** at 45.7 °C in THF-d_8 occurred with a k_{obs} of 5.82×10^{-4} ($\pm$ 0.04×10^{-4}) s^{-1}. A

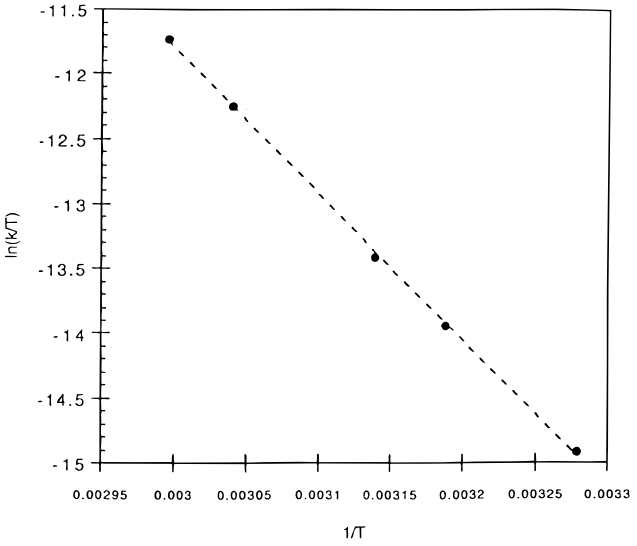

Figure 6. Eyring plot (30−60 °C) for the reaction of **2** with styrene.

Scheme 4

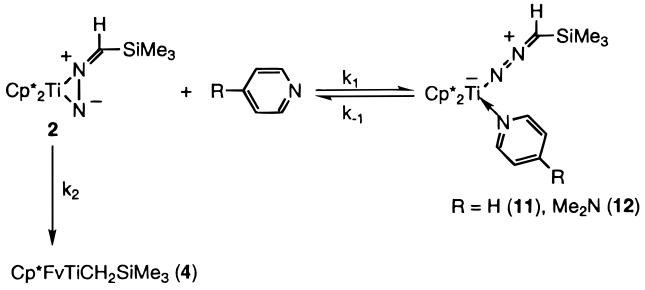

detailed study of the electronic factors influencing dinitrogen loss from phenyl-substituted diazoalkane complexes will be the subject of a future publication.[32]

Reaction of 2 with Lewis Bases. Retention of N_2. In an attempt to intercept any intermediates in the thermolysis of **2** to **4**, the reaction was run in the presence of 5 equiv of trimethylphosphine. The added trimethylphosphine had no effect on the reaction rate, and formation of **4** was observed with no detectable intermediates. In contrast, when excess pyridine or *p*-(dimethylamino)pyridine (DMAP) is added to a benzene-d_6 solution of **2**, a color change from green to purple is observed. The ^{1}H NMR spectra of the purple solutions show the presence of **2** and a new compound, assigned as the pyridine (**11**) or DMAP (**12**) adduct of **2** (Scheme 4). The resonances for free and bound pyridine are coalesced at room temperature, indicating that exchange of free and bound pyridine is rapid on the NMR time scale. Removal of the volatile materials under dynamic vacuum leaves a green powder which, when redissolved in benzene-d_6, gives a ^{1}H NMR spectrum of pure **2**, confirming that the base binds reversibly. Solutions of **11** and **12** decompose slowly at 25 °C to give fulvene complex **4** and free pyridine or DMAP. The rate of formation of **4** is markedly slower in the presence of pyridine or DMAP; however, **11** and **12** could not be isolated due to loss of pyridine or DMAP. It seems reasonable to assign these complexes as the pyridine or DMAP adduct of an end-on diazoalkane complex (Scheme 4), since a similar compound, $Cp_2Ti(N_2CPh_2)(PMe_3)$ (**13**) (Scheme 5) is known. It is unlikely that **11** and **12** still possess side-bound diazoalkane ligands with the pyridine or DMAP coordinated to the metal, since the bulky decamethyltitanocene

(32) Kaplan, A. W.; Polse, J. L.; Ball, G. E.; Andersen, R. A.; Bergman, R. G. Submitted for publication.

Scheme 5

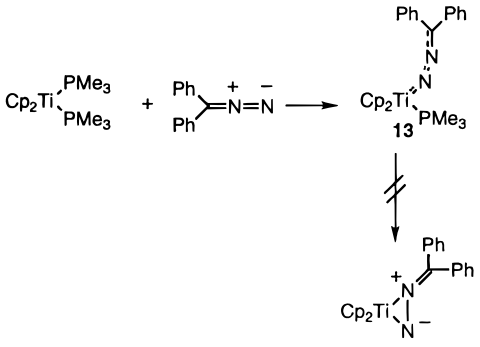

Scheme 6

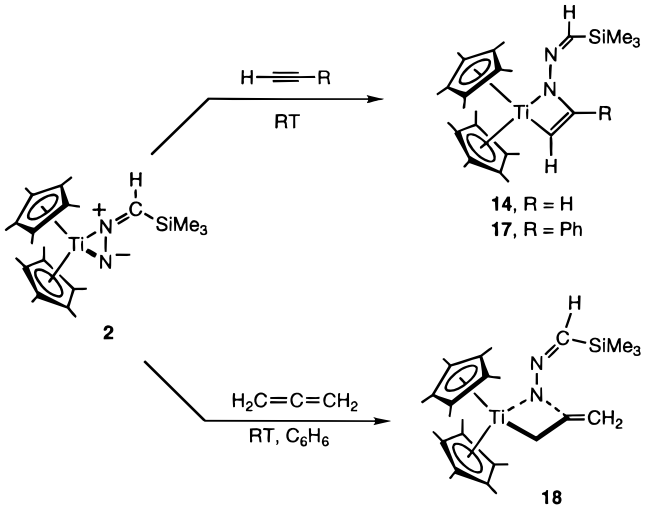

Scheme 7

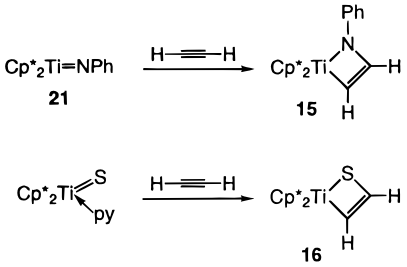

fragment strongly disfavors coordination of three ligands in the metallocene wedge.

Reactivity toward Alkynes and Allene. Synthesis and Structure of Azatitanacycle Complexes. Exposing a deep green benzene solution of **2** to a stream of dry acetylene gas results in an immediate color change to deep red. Removal of the volatile materials followed by crystallization from hexanes (−50 °C) yields red crystals of a new complex, identified as azametallacyclobutene **14** (Scheme 6). The reaction time is critical since longer reaction times led to precipitation of a black solid which is presumed to be polyacetylene. Retention of dinitrogen in **14** was confirmed by elemental analysis and mass spectroscopy. In addition to two singlets for the trimethylsilyl group and Cp* methyl groups, the ^{1}H NMR spectrum of **14** displays two doublets (^3J = 9.4 Hz) at 7.29 and 6.52 ppm attributable to the methine protons on the metallacycle ring. This compares favorably with the methine resonances in related aza- (**15**) and thiatitanacyclobutene (**16**) complexes (Scheme 7) (**15**: δ 7.02, 7.08 ppm, ^3J = 9 Hz; **16**: δ 6.52, 7.42 ppm, ^3J = 9.9 Hz).[33,34] The methine proton of the diazoalkane moiety is shifted to 6.33 ppm. The ^{13}C NMR spectrum displays two resonances at 180.2 and 133.3 ppm which were assigned as methine carbons using standard DEPT pulse sequences. The resonance at 180.2 is characteristic of an sp^2 carbon bound to Ti.[35] If the diazoalkane complex had acted as a base to deprotonate the acetylene and give a metal acetylide complex, neither the strong coupling in the ^{1}H NMR spectrum nor the two methine resonances in the ^{13}C NMR spectrum would be expected.

Treatment of a benzene solution of **2** with 1 equiv of phenylacetylene gives a red solution from which crystals of azametallacyclobutene **17** (Scheme 6) can be isolated in 64% yield. Retention of dinitrogen was confirmed by mass spectroscopy and elementary analysis. The ^{1}H NMR spectrum of **17** shows singlets for the metallacycle and diazoalkane methine protons at 6.34 and 2.99 ppm, respectively. The ^{13}C NMR spectrum shows a methine resonance at 192.3 ppm, consistent with an sp^2 carbon bound to Ti. The chemical shifts for the metallacyclobutene ring are comparable to those reported for related titanium oxametallacyclobutene complexes.[36] In addition, the shift is quite similar to that of the α-proton in **14** (180.2 ppm). As discussed above for **14**, formulation of **17** as an acetylide complex resulting from deprotonation of the alkynyl proton by the acidic nitrogen of **2** is inconsistent with the presence of a methine carbon resonance at >180 ppm. In addition, the IR spectrum shows no N−H or acetylide C≡C stretches as would be expected from an amide acetylide complex.

Treatment of **2** with allene at −195 °C results in an immediate color change from green to red upon warming to room temperature. Removal of the solvent gives a red powder which may be crystallized from hexanes at −50 °C to give Cp*$_2$Ti(NN=CHSiMe$_3$)C(CH$_2$)CH$_2$ (**18**) in 78% yield (Scheme 6). Retention of dinitrogen was confirmed by elemental analysis and mass spectroscopy. In addition to two singlets for the trimethylsilyl group and Cp* methyl groups, the ^{1}H NMR spectrum of **18** displays two doublets (^3J = 1.9 Hz) at 4.77 and 3.78 ppm corresponding to the exocyclic protons on the metallacycle ring. The methylene protons α to the titanium center resonate at 2.62 ppm, and the methine proton on the diazoalkane fragment is shifted to 6.23 ppm. The equivalent Cp* methyl groups and ring methylene protons are consistent with either a planar azametallacyclobutane ring or a puckered ring undergoing a rapid ring flip. Although the puckered structure of the metallacycle ring was determined by X-ray crystallography (vide infra), the resonances for the Cp* and methylene protons remained singlets down to − 70 °C. To determine the regiochemistry of azametallacyclobutane complex **18**, a ^{1}H−^{1}H NOESY spectrum was acquired as described in the Experimental Section. The two possible isomers have the exocyclic double bond α or β to the metal center. The proton on the diazoalkane moiety and the Me$_3$Si group both showed cross-peaks to the exocyclic protons, but not to the ring protons. This indicates that the exocyclic double bond is β to the metal center.

To confirm the NMR assignment of **18**, a single-crystal X-ray diffraction study was undertaken. The structure was solved by direct methods and refined using standard least-squares and

(33) Sweeney, Z. K.; Bergman, R. G. Unpublished results.
(34) Polse, J. L.; Andersen, R. A.; Bergman, R. G. Manuscript in preparation.
(35) Doxsee, K. M.; Juliette, J. J. J.; Weakley, T. J. R.; Zientara, K. *Inorg. Chim. Acta* **1994**, *222*, 305 and references therein.
(36) Polse, J. L.; Andersen, R. A.; Bergman, R. G. *J. Am. Chem. Soc.* **1995**, *117*, 5393.

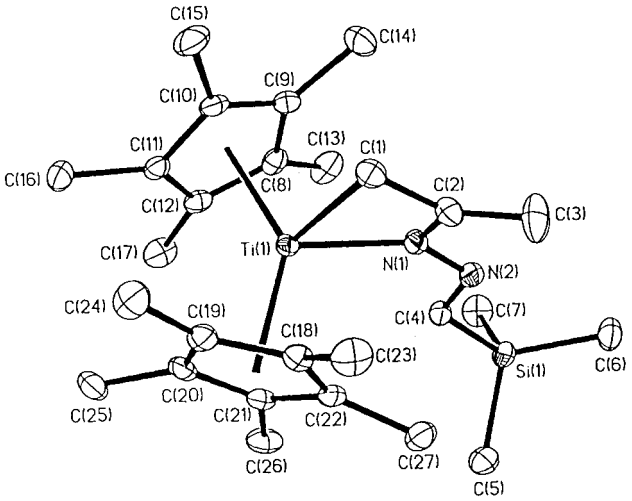

Figure 7. ORTEP diagram of $Cp^*_2Ti(N(N{=}C(H)SiMe_3)C(CH_2)CH_2)$ (**16**).

Table 4. Selected Bond Distances (Å) and Angles (deg) for **18**

Ti−N1	2.065(2)	Ti−C1	2.187(2)
Ti−C101	2.1308(4)	Ti−C102	2.1209(4)
C1−C2	1.509(3)	N1−C2	1.388(3)
C2−C3	1.352(4)	N1−N2	1.374(2)
N2−C4	1.294(3)		
N1−Ti−C1	66.41(8)	C101−Ti−C102	138.61(2)
N1−Ti−C101	108.55(5)	N1−Ti−C102	108.58(5)
C1−Ti−C101	104.73(7)	C1−Ti−C102	106.37(7)
Ti−N1−C2	95.8(1)	Ti−C1−C2	87.5(1)
N1−C2−C1	107.0(2)	Ti−N1−N2	143.5(1)
N1−C2−C3	127.3(3)	C1−C2−C3	125.5(2)
N2−N1−C2	117.3(2)		

Fourier techniques. Crystal and data collection parameters are shown in Table 1 and details of the structure determination are given in the Experimental Section. Positional and thermal parameters are given as Supporting Information. An ORTEP diagram of **18** is shown in Figure 7. Table 4 provides intramolecular bond lengths and angles for this compound. As expected, the exocyclic double bond is β to the metal center. The structure also shows that the trimethylsilyl group is directed out of the Cp* wedge. The Ti−C1 distance was found to be 2.187(2) Å, within the typical range (2.14−2.21 Å) for Ti−$C_{sp}3$ bonds.[31] The ring deviates slightly from planarity; the dihedral angle between the planes formed by Ti(1), C(1), and N(1), and the plane formed by C(2), C(1), and N(1) is 161°. Ti(1) lies 0.645 Å out of the least-squares plane formed by N(1), C(1), C(2), and C(3).

To study the generality of its cycloaddition reactions, complex **2** was treated with N_2O, which is isoelectronic with allene. When **2** was exposed to 1 equiv of N_2O in benzene, the solution turned from dark green to a deep red-black. Removal of the volatile materials and crystallization from Et_2O (−50 °C) gave crystals of **19** (Scheme 8). Mass spectroscopy and elemental analysis confirmed that **19** possessed an elemental composition corresponding to retention of 1 equiv of N_2, presumably from the diazoalkane fragment. This rules out the possibility that **19** is the product of a [2 + 2] cycloaddition of **2** with N_2O as observed for allene. Examination of the ^1H and ^{13}C NMR spectra of **19** showed that it did not contain a five-membered metallacycle (Scheme 8), the result from oxygen atom transfer. The ^1H NMR spectrum shows a broad one-proton singlet at 8.09 ppm and a singlet for equivalent Cp* methyl groups. Examination of the ^{15}N-filtered ^1H NMR spectrum of **19** showed that the resonance at 8.09 possesses a 68.2 Hz ^1J coupling to ^{15}N. In addition to resonances for the Me_3Si and Cp* groups, the ^{13}C NMR spectrum shows only one other resonance at 177.1 ppm, assigned as a quaternary carbon by standard DEPT pulse sequences. In addition, the IR spectrum of **19** shows a stretch at 3290 cm^{-1} consistent with a NH stretch. On the basis of the above data, complex **19** is assigned the structure shown in Scheme 8. Interestingly, **19** also is obtained from oxotitanium complex $Cp^*_2Ti(O)py$ (**20**)[37] and $Me_3SiC(H)N_2$.

Discussion

Synthesis and Structure of $Cp^*_2Ti(N_2CHSiMe_3)$ (2). As described in the Results section, treatment of **1** with (trimethylsilyl)diazomethane results in clean formation of diazoalkane complex **2** and ethylene (eq 3). The retention of dinitrogen was somewhat unexpected in light of similar reactions of **1** toward oxygen-atom and nitrene donors. As described previously, **1** reacts with N_2O and organic azides to liberate ethylene and dinitrogen, giving $Cp^*_2Ti(O)py$ (**20**)[38] and $Cp^*_2Ti{=}NR$ (**21**), respectively (Scheme 9).[36,39] By analogy to the oxygen- and nitrene-transfer reactions, carbene complex **22** (Scheme 9) would be the expected product of the reaction of a diazoalkane with **1**. If N_2O[40−45] and azide complexes[46,47] similar to **2** are formed on the reaction path to **20** and **21**, they lose nitrogen much more rapidly than does **2**. Complex **2** liberates dinitrogen slowly to generate what is presumed to be a carbene complex intermediate, which then reacts with a variety of substrates (vide infra). It is possible that the instability of the carbene complex leads to a higher barrier for N_2 loss than was observed for the reactions of **1** with N_2O and organic azides.

A possible mechanism for the formation of **2** is outlined in Scheme 10. The mechanism postulates an initial insertion of the diazoalkane into the Ti−C bond of **1** to give an azametallacyclobutane complex (**23**). A similar insertion of diphenyldiazomethane into the Zr−C bond of $Cp^*_2Zr(\eta^2\text{-PhC}{\equiv}\text{CPh})$ to give an azametallacyclobutene complex has been described previously (eq 4).[48] The intermediate azametallacyclobutane

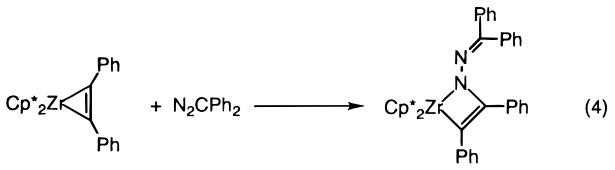

(4)

23 can then undergo a cycloreversion reaction similar to the one discussed for $Cp^*_2Ti(N(Ph)CH_2CH_2)$ (eq 5)[34] to liberate

(37) Smith, M. R., III; Matsunaga, P. T.; Andersen, R. A. *J. Am. Chem. Soc.* **1993**, *115*, 7049.
(38) The reaction of **1** with N_2O must be run in the presence of excess pyridine, since **16** is only stable as a pyridine adduct.
(39) Smith, M. R., III; Ball, G. E.; Andersen, R. A. Manuscript in preparation.
(40) Armor, J. N.; Taube, H. *J. Am. Chem. Soc.* **1969**, *91*, 6874.
(41) Bottomley, F.; Crawford, J. R. *J. Chem. Soc., Chem. Commun.* **1971**, 200.
(42) Bottomley, F.; Crawford, J. R. *J. Am. Chem. Soc.* **1972**, *94*, 9092.
(43) Diamantis, A. A.; Sparrow, G. J. *J. Chem. Soc., Chem. Commun.* **1970**, 819.
(44) Diamantis, A. A.; Sparrow, G. J.; Snow, M. R.; Norman, T. R. *Aust. J. Chem.* **1975**, *28*, 1231.
(45) Tuan, D. F.; Hoffman, R. *Inorg. Chem.* **1985**, *24*, 871.
(46) Fickes, M. G.; Davis, W. M.; Cummins, C. C. *J. Am. Chem. Soc.* **1995**, *117*, 6384.
(47) Proulx, G.; Bergman, R. G. *J. Am. Chem. Soc.* **1995**, *117*, 6382.
(48) Vaughan, G. A.; Hillhouse, G. L.; Rheingold, A. L. *J. Am. Chem. Soc.* **1990**, *112*, 7994.

Scheme 8

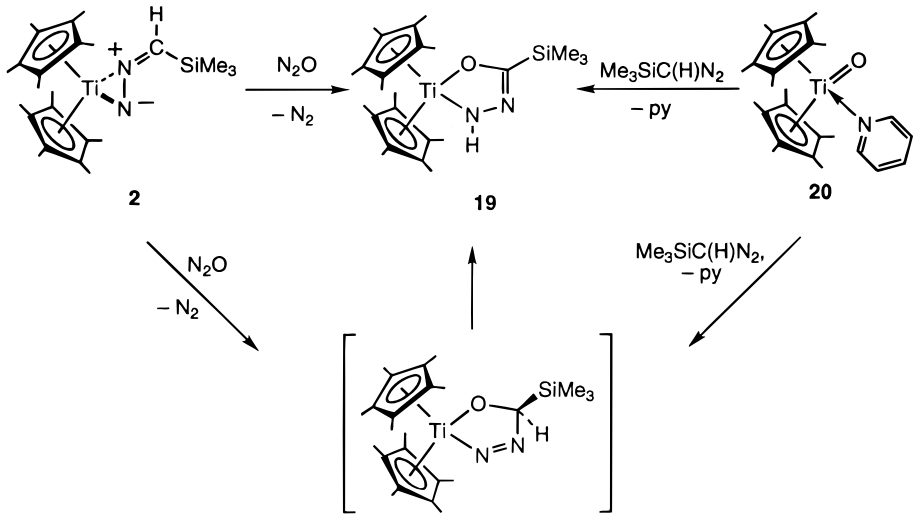

Scheme 9

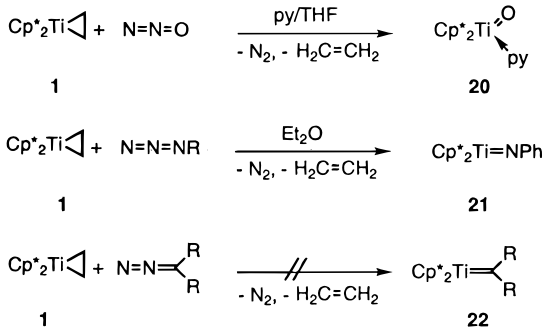

Scheme 10

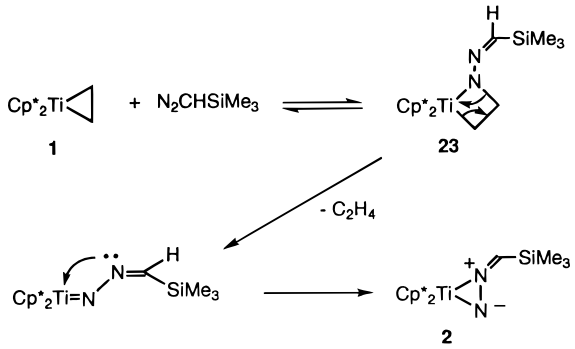

ethylene; coordination of the second nitrogen forms **2**.

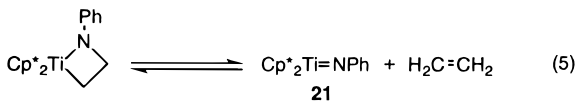

It is also possible to envision a mechanism in which ethylene dissociation precedes diazoalkane coordination. Such a mechanism can be discounted, however, since ethylene does not dissociate from **1** to give free Cp^*_2Ti.[21]

Thermal Loss of Dinitrogen from 2. Formation of $Cp^*FvTiCH_2SiMe_3$ (4). As was noted above, in the absence of traps **2** loses dinitrogen thermally to give fulvene complex **4** (Scheme 2). The mild conditions under which **2** loses dinitrogen are surprising, since (as pointed out earlier) few isolable diazoalkane complexes release dinitrogen.[2–4] For example, the related titanium diazoalkane complexes $Cp_2Ti(DEDM)$ (**3**) (Scheme 1) and $Cp_2Ti(N_2CPh_2)(PMe_3)$ (**13**) (Scheme 5) do not lose dinitrogen thermally or photochemically.[15,49] It is possible that an open coordination site at the metal center is required for N_2 loss to occur and that the tightly bound ancillary ligands of **3** and **13** render them inert to this reaction.

There are several other examples of isolated diazoalkane complexes that lose dinitrogen to give metal carbene complexes.[2,8–10,12,16,50] For example, the bridging molybdenum diazoalkane complex **24** loses dinitrogen thermally to give carbene complex **25** (eq 6).[8] The authors postulate that carbene

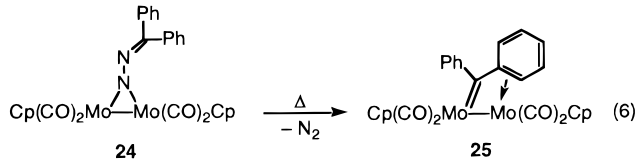

formation occurs via a cyclic transition state in which the diazoalkane and the dimolybdenum center form a five membered ring which then extrudes N_2.[8] Although the intimate mechanism of dinitrogen loss from **2** is still largely unknown, we have been able to obtain some preliminary information about it from a kinetic study of the reaction of **2** with styrene (vide infra), and an in-depth study of the electronic factors involved in this step is underway.[32]

Reaction of 2 with α-Olefins. Mechanistic Discussion. We have carried out a kinetic study of the reaction of **2** with styrene in order to obtain further information on the mechanism of nitrogen loss and metallacycle formation. The kinetic study was carried out as described in the Results Section and Experimental Section. The reaction was first order in [**2**], and the rate showed no dependence on styrene concentration. Monitoring the reaction at a variety of temperatures between 30 and 60 °C allowed measurement of the activation parameters $\Delta H^{\ddagger} = 22.5 \pm 0.3$ kcal/mol, $\Delta S^{\ddagger} = -3.1 \pm 1.0$ eu, and $\Delta G^{\ddagger} = 23.4 \pm 0.4$ kcal/mol (calculated at 25 °C). Because there is no rate dependence on styrene concentration, any mechanism that invokes an attack of the alkene prior to or during the rate determining step of the reaction can be ruled out.

We favor a mechanism (Scheme 11) in which the rate-limiting step involves rearrangement to lose dinitrogen and give carbene

(49) For examples of other structurally characterized Ti diazoalkane complexes, see: Kool, L. B.; Rausch, M. D.; Alt, H. G.; Herberhold, M.; Hill, A. F.; Thewalt, U.; Wolf, B. *J. Chem. Soc., Chem. Commun.* **1986**, 408. See also ref 15.

Scheme 11

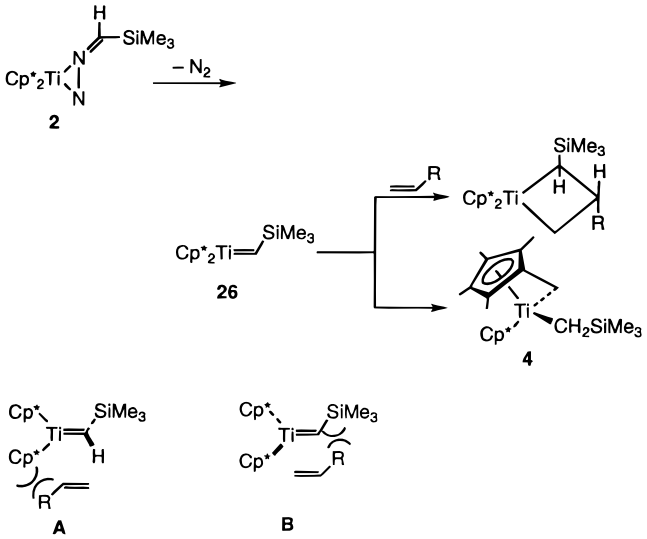

complex intermediate **26**. Complex **26** can then either react with the C−H bond of the Cp* ligand to give **4**, or it can undergo a [2 + 2] cycloaddition with alkenes to give metallacyclobutanes. The reaction of **26** with a Cp* methyl group to give **4** is precisely analogous to the Cp* C−H activation in transient $Cp^*_2Ti{=}CH_2$ reported by Bercaw (Scheme 2).[24] This mechanism is consistent with the lack of rate dependence on alkene concentration, and it also accounts for the observed regiochemistry of the metallacyclobutanes. Approach of the α-olefin to the carbene in a manner that would place the substituent α to the metal center (transition state **A**, Scheme 11) is disfavored due to unfavorable steric interactions with the Cp* rings. Similarly, the olefin approaches in such a way as to minimize contact between the olefinic substituent and the trimethylsilyl group of the carbene (transition state **B**, Scheme 11), and therefore the trans-α,*β*-disubstituted isomer is formed.

There are several possibilities for the structure of the transition state leading to dinitrogen loss from **2**. One possibility that is often invoked in the reactivity of diazoalkanes to form metal carbene complexes is rearrangement to an intermediate in which the diazoalkane coordinates through the C=N rather than the N=N bond. Then, in a reaction that is analogous to release of CO from metal ketene complexes, the dinitrogen is extruded to form carbene intermediate **26**. Another possibility involves coordination of carbon to titanium in a four-membered ring that then loses dinitrogen. The latter pathway would be consistent with the lack of a solvent effect on the reaction, since it possesses no formal charge separation. These possible transition states must be treated as conjecture, since we have little direct information on the dinitrogen extrusion step. A detailed study of substituent effects on dinitrogen extrusion from aryl-substituted diazoalkane complexes is currently in progress.[32]

Attempts to trap carbene intermediate **26** with the Ti=C bond intact have not yet been successful.[51] Bases such as pyridine and DMAP add to **2** to give adducts **11** and **12** which decompose to **4** (Scheme 4). Interestingly, the rate of formation of **4** is markedly slower in the presence of pyridine or DMAP, undoubtedly because **2** is "tied up" by formation of substantial amounts of **11** or **12** as a result of the rapid equilibrium between **11** or **12** and **2**. This suggests that **11** and **12** decompose via free **2** and is consistent with our supposition that dinitrogen loss requires a vacant coordination site at titanium (vide supra). We have also attempted to induce dinitrogen loss photochemically at low temperatures. Irradiation of **2** through Pyrex glass at −10 °C alone or in the presence of pyridine gave no reaction. Irradiation of **2** through quartz led to decomposition to an intractable mixture of products.

Reactions of 2 that Retain Nitrogen. Azametallacycle Formation. As mentioned in the Results section, when treated with terminal alkynes, **2** undergoes cyclization reactions that proceed with retention of N_2 to give azametallacyclobutene complexes. Hillhouse and co-workers have previously described a zirconium azametallacyclobutene complex in which the fragments are assembled in reverse order.[52] The alkyne complex $Cp^*_2Zr(PhC{\equiv}CPh)$ reacts with diphenyldiazomethane to form the metallacycle shown in eq 4. The cyclization reactions with alkynes are quite similar to those observed for group IV imido and oxo complexes.[53−63] In particular, the reaction of **2** with acetylene to form **14** is similar to the reaction of the imido complex **21** with acetylene to form metallacycle **15** (Scheme 7).[34] In addition, the reactions of **2** with Lewis bases described above are analogous to the reaction of transient group IV imido complexes with Lewis bases to form stable adducts.[55,56,65] This suggests that at least in solution, there is some imide-like character to the bonding in **2**, which can be illustrated as shown:

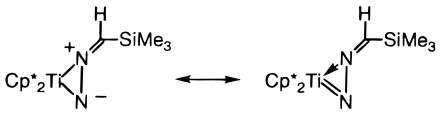

The reaction of **2** with phenylacetylene yields azametallacyclobutene complex **17** (Scheme 6). Despite its similarity to **14**, the formation of **17** was somewhat unexpected, since the analogous reaction of imido complex **21** with phenylacetylene yields the amide−acetylide rather than the metallacyclobutene product (Scheme 12).[34] Oxotitanium complex **20** reacts with a variety of terminal alkynes to give the corresponding oxametallacyclobutene complexes as shown in Scheme 12.[36] The oxametallacyclobutene complexes rearranged to the more thermodynamically stable hydroxo acetylide complexes. To determine whether it would undergo a similar rearrangement, a benzene-d_6 solution of **17** was heated to 45 °C for 7 days, during

(50) Cowie, M.; McKeer, I. R.; Loeb, S. J.; Gauthier, M. D. *Organometallics* **1986**, *5*, 860.
(51) Petasis, N. A.; Staszewski, J. P.; Fu, D. K. *Tetrahedron Lett.* **1995**, *36*, 3619.
(52) Vaughan, G. A.; Hillhouse, G. L.; Rheingold, A. L. *J. Am. Chem. Soc.* **1990**, *112*, 7994−8001.
(53) Meyer, K. E.; Walsh, P. J.; Bergman, R. G. *J. Am. Chem. Soc.* **1995**, *117*, 3749.
(54) Walsh, P. J.; Baranger, A. M.; Bergman, R. G. *J. Am. Chem. Soc.* **1992**, *114*, 1708.
(55) Mountford, P. *Chem. Commun.* **1997**, 2127.
(56) Walsh, P. J.; Hollander, F. J.; Bergman, R. G. *J. Am. Chem. Soc.* **1988**, *110*, 8729.
(57) Housmekerides, C. E.; Ramage, D. L.; Kretz, C. M.; Shontz, J. T.; Pilato, R. S.; Geoffroy, G. L.; Rheingold, A. L.; Haggerty, B. S. *Inorg. Chem.* **1992**, *31*, 4453.
(58) Carney, M. J.; Walsh, P. J.; Hollander, F. J.; Bergman, R. G. *J. Am. Chem. Soc.* **1989**, *111*, 8751.
(59) Carney, M. J.; Walsh, P. J.; Hollander, F. J.; Bergman, R. G. *Organometallics* **1992**, *11*, 761.
(60) Carney, M. J.; Walsh, P. J.; Bergman, R. G. *J. Am. Chem. Soc.* **1990**, *112*, 6426.
(61) Walsh, P. J.; Hollander, F. J.; Bergman, R. G. *Organometallics* **1993**, *12*, 3705.
(62) Meyer, K. E.; Walsh, P. J.; Bergman, R. G. *J. Am. Chem. Soc.* **1994**, *116*, 2669.
(63) Meyer, K. E.; Walsh, P. J.; Bergman, R. G. *J. Am. Chem. Soc.* **1995**, *117*, 974.
(64) Bennett, J. L.; Wolczanski, P. T. *J. Am. Chem. Soc.* **1994**, *116*, 2179.
(65) Cummins, C. C.; Baxter, S. M.; Wolczanski, P. T. *J. Am. Chem. Soc.* **1988**, *110*, 8731.

Scheme 12

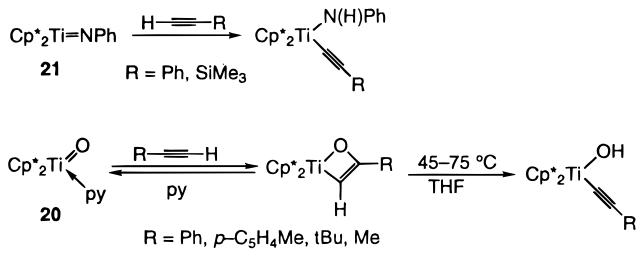

Scheme 13

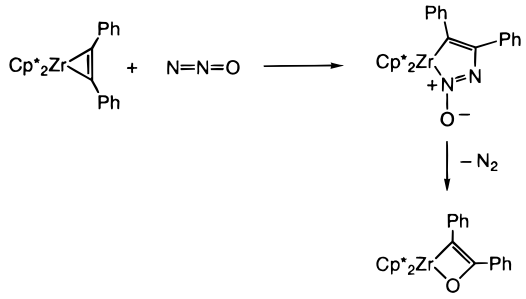

which time it decomposed to an intractable mixture of products. Apparently, small changes in the nature of the titanium−heteroatom bond profoundly influence the relative stability of the isomeric metallacyclobutene and acetylide complexes.

Diazoalkane complex **2** also forms an azametallacyclobutane complex (**18**) when treated with allene; the product is stable up to 45 °C. In contrast, when the imido complex **21** is treated with allene, a metallacycle is observed spectroscopically,[66] but is not stable to isolation. Oxotitanium complex **20** reacts with allene to give an analogous oxametallacyclobutane complex (**27**, eq 7).[67] Complex **27** shows regiochemistry identical to that of

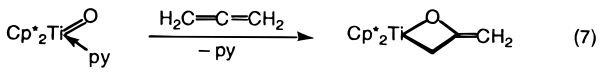

(7)

20 **27**

18 (the exocyclic double bond is β to the metal center), and in the solid state **18** shows a slight pucker of the metallacycle ring. However, flipping of the ring is fast in solution, as demonstrated by a low-temperature ^{1}H NMR study which showed singlets for the Cp* and methylene resonances down to −70 °C as is true for complex **27**.[67]

Treatment of diazoalkane complex **2** with N_2O yields metallacycle **19**, where N_2O has formally transferred an oxygen atom, and a hydrogen shifts from carbon to nitrogen (Scheme 8). Hillhouse and co-workers observed that the alkyne complex Cp*$_2$Zr(η^2-PhC≡Ph) reacts with N_2O to affect formal transfer of the oxygen atom and the intermediate demonstrating insertion of N_2O into the Zr−C(alkyne) bond was isolated (Scheme 13).[48] We observe no intermediate in the formation of **19**, but it seems reasonable that N_2O inserts before the extrusion of N_2 as in the zirconium system. Also, as mentioned in the Results section, complex **19** can also be formed by the reaction of oxotitanium complex **20** with (trimethylsilyl)diazomethane. To obtain the same complex from the reaction with **2** and N_2O, the released N_2 almost certainly comes from the N_2O fragment.

Conclusions

We have synthesized a novel side-bound diazoalkane complex of titanium, Cp*$_2$Ti(N_2CHSiMe$_3$) (**2**), from Cp*$_2$Ti(C_2H_4) (**1**) and trimethylsilyldiazomethane. Unlike most isolable diazoalkane complexes, **2** releases dinitrogen under mild conditions to give Cp*FvTiCH$_2$SiMe$_3$ (**4**). Thermolysis of **2** in the presence of α-olefins leads to the trans-α,β-disubstituted metallacyclobutane complexes **6**−**9**. The regiochemistry of the metallacyclobutane complexes was determined by a combination of one- and two-dimensional NMR techniques and confirmed by X-ray crystallography in the case of Cp*$_2$Ti(CH(SiMe$_3$)CH(Me)CH$_2$) (**8**). A kinetic study of the reaction of **2** with styrene supports a mechanism involving a transient carbene complex which is trapped by styrene to give the metallacyclobutane Cp*$_2$Ti(CH(SiMe$_3$)CH(Ph)CH$_2$) (**7**). Addition of Lewis bases pyridine and DMAP to **2** do not trap this transient carbene complex, but form reversible adducts with the metal center which slows the formation of **4**. It seems likely that the open coordination site in **2** is necessary for N_2 loss to occur, and this may be a general requirement for N_2 loss from metal diazoalkane complexes.

We have also shown that **2** has a varied reactivity that involves the retention of N_2. The coordination mode of the diazoalkane fragment may be changed by the addition of Lewis bases. Terminal acetylenes and allene react with **2** to form azametallacyclobutane complexes **14**, **17**, and **18**. N_2O formally transfers an oxygen atom to **2** to form titanacycle **19**. The reactivity pattern of these reactions is similar to that exhibited by complexes containing Ti═X multiple bonds, and suggests that the bonding in **2** can be described as possessing both imido−olefin−adduct components.

Experimental Section

General Methods. Unless otherwise noted, all reactions and manipulations were carried out in dry glassware under a nitrogen or argon atmosphere at 20 °C in a Vacuum Atmospheres 553-2 drybox equipped with a MO-40-2 inert gas purifier, or using standard Schlenk techniques. The amount of O_2 in the drybox atmosphere was monitored with a Teledyne model no. 316 trace oxygen analyzer. Some reactions were carried out in thick-walled glass vessels fused to vacuum stopcocks; these are referred to in the procedures as glass bombs. The other instrumentation and general procedures used have been described previously.[53]

Unless otherwise specified, all reagents were purchased from commercial suppliers and used without further purification. Dimethyoxybenzene and 4-(dimethylamino)pyridine (DMAP) were sublimed prior to use. Styrene was stirred over activated 4 Å molecular sieves, vacuum distilled, and then stored at −50 °C in contact with activated 4 Å molecular sieves. Pyridine was distilled from CaH_2 or sodium under nitrogen and was stored in contact with activated 4 Å molecular sieves. Trimethylphosphine was distilled from sodium just prior to use. Acetylene gas was purified by passage through two −78 °C traps separated by a concentrated H_2SO_4 trap. Pentane and hexanes (UV grade, alkene free) were distilled from sodium benzophenone ketyl/tetraglyme under nitrogen. Cyclohexane was distilled from calcium hydride under nitrogen. Deuterated solvents for NMR experiments were dried in the same way as their protiated analogues but were vacuum transferred from the drying agent. Cp*$_2$Ti(C_2H_4) was prepared by the literature method,[21] except that Cp*$_2$TiCl was used instead of Cp*$_2$TiCl$_2$.[68]

NMR Spectroscopy. NMR experiments were performed on a Brucker AMX spectrometer resonating at 300.13 MHz for ^{1}H and 75.42 MHz for ^{13}C that was equipped with an inverse probe. One-dimensional ^{13}C{^{1}H} spectra and DEPT spectra were recorded on a Brucker AMX spectrometer resonating at 400 MHz for ^{1}H and 100 MHz for ^{13}C that was equipped with a QNP probe. ^{15}N-filtered ^{1}H NMR spectra were obtained using a pulse sequence similar to that described by Griffey,[69]

(66) Polse, J. L.; Bergman, R. G. Polse, J. L.; Bergman, R. G. Unpublished results.

(67) Schwartz, D. J.; Smith, M. R., III.; Andersen, R. A. *Organometallics* **1996**, *15*, 1446.

(68) Pattiasina, J. W.; Heeres, H. J.; Von Bolhuis, F.; Meetsma, A.; Teuben, J. H. *Organometallics* **1987**, *6*, 1004.

(69) Bax, A.; Griffey, R. H.; Hawkins, B. L. *J. Magn. Reson.* **1988**, *55*, 301.

modified to give only the one-dimensional ^{1}H NMR spectrum. All two-dimensional experiments were acquired between 295 and 300 K. NOESY spectra were acquired in phase-sensitive mode using the Brucker pulse program noesytp. A shifted sine-bell window function was applied to the raw data set in both dimensions.

Cp*$_2$TiN$_2$CHSiMe$_3$ (2). (Trimethylsilyl)diazomethane (300 μL of a 2 M solution in hexanes, 0.600 mmol) was added via syringe to a stirred solution of **1** (209 mg, 0.602 mmol) in C_6H_6 (10 mL). Gas evolution ensued, and the solution turned from lime to forest green within 30 s. The solution was stirred for 10 min, and the volatile materials were removed under vacuum. The dark green powder was extracted into hexanes and filtered. The volume of the filtrate was reduced to 3 mL, and cooled to −80 °C to yield **2** as dark green blocky crystals (169 mg, 65%). IR (Nujol): 2723 (w), 1894 (br,w), 1324 (m), 1232 (m), 1091 (m), 1022 (m), 848 (s), 703 (m) cm^{-1}. ^{1}H NMR (C_6D_6): δ 0.44 (s, 9H), 1.71 (s, 30H), 4.11 (s, 1H) ppm. ^{13}C{^{1}H} NMR (C_6D_6): δ −0.35 (CH_3), 11.35 (CH_3), 99.9 (CH), 122.2 (C) ppm. MS-EI m/z = 433 [M$^+$]. Anal. Calcd for $C_{24}H_{40}N_2SiTi$: C, 66.62; H, 9.34; N, 6.48. Found: C, 66.31; H, 9.30; N, 6.65.

Cp*FvTiCH$_2$SiMe$_3$ (4). A glass bomb was charged with crystals of **2** (74.3 mg, 0.172 mmol) and 10 mL of C_6H_6. The solution was stirred for 2 d at 25 °C, during which time it turned from forest green to blue-green. The volatile materials were removed under vacuum and the blue-green powder was extracted into hexanes and filtered. The volume of the filtrate was reduced to 1 mL under vacuum and cooled to −50 °C to yield aquamarine crystals of **4** (58.7 mg, 84.3%). IR (Nujol): 2721 (w), 1238 (m), 1076 (w), 1022 (m), 881(m), 847 (s), 787 (s), 717 (m), 667 (m) cm^{-1}. ^{1}H NMR (C_6D_6): δ −1.29 (d, ^2J = 10.8 Hz, 1H), 0.15 (s, 9H), 0.21 (d, ^2J = 10.8 Hz, 1H), 1.26 (s, 3H), 1.29 (d, ^2J = 4.0 Hz, 1H), 1.41 (s, 3H), 1.80 (s, 15H), 1.83 (s, 3H), 2.02 (d, ^2J = 4.0 Hz, 1H), 2.20 (s, 3H). ^{13}C{^{1}H} NMR (C_6D_6): δ 6.1 (CH_3), 10.8 (CH_3), 11.4 (CH_3), 12.3 (CH_3), 12.5 (CH_3), 15.6 (CH_3), 45.8 (CH_2), 76.1 (CH_2), 118.9 (C), 120.0 (C), 125.1 (C), 125.9 (C), 126.6 (C), 130.1 (C) ppm. MS-EI m/z = 405 [M$^+$]. Anal. Calcd for $C_{24}H_{40}SiTi$: C, 71.24; H, 9.98. Found: C, 71.18; H, 10.24.

Cp*$_2$Ti(CHSiMe$_3$CH$_2$CH$_2$) (6). A glass bomb was charged with **1** (111 mg, 0.320 mmol) in 10 mL of C_6H_6. (Trimethylsilyl)-diazomethane (160 μL of a 2 M solution in hexanes) was added using a syringe. The bomb was quickly closed. The solution turned from lime to dark green immediately. The bomb was immersed in a 45 °C bath for 6 h, during which time the green solution gradually turned bright red. The volatile materials were removed under vacuum, and the red oily residue was extracted into diethyl ether and cooled to −50 °C for 12 h to yield dark red crystals of **6** (84.4 mg, 60.9%). IR (Nujol): 2721 (m), 2049 (w), 1240 (s), 1020 (m), 887 (m), 829 (s), 665 (m) cm^{-1}. ^{1}H NMR (C_6D_6): δ −0.53 (m, 1H), 0.28 (s, 9H), 1.06 (m, 1H), 1.54 (m, 1H), 1.70 (s, 15H), 1.73 (s, 15H), 1.77 (m, 2H) ppm. ^{13}C{^{1}H} (C_6D_6): δ 3.9 (CH_3), 5.8 (CH_2), 12.2 (CH_3), 12.3 (CH_3), 71.1 (CH_2), 73.2 (CH), 116.9 (C), 117.3 (C) ppm. Anal. Calcd for $C_{26}H_{44}$-SiTi: C, 72.17; H, 10.27. Found: C 71.78; H, 10.34.

Cp*$_2$Ti(CHSiMe$_3$CHPhCH$_2$) (7). A solution of styrene (98.1 mg, 0.942 mmol) in C_6H_6 (2 mL) was added to a stirred solution of **2** (54.6 mg, 0.126 mmol) in C_6H_6 (10 mL). The solution was stirred for 48 h at 25 °C, during which time it turned from green to red. The volatile materials were removed under vacuum, and the resulting red powder crystallized from diethyl ether at −50 °C to give red crystals of **7** (55.2 mg, 86.1%). ^{1}H NMR (C_6D_6): δ 0.13 (s, 9H), 1.36 (m, 2H), 1.65 (m, 1H), 1.77 (s, 15H), 1.79 (s, 15H), 1.99 (d, ^3J = 14 Hz, 1H), 7.8 (m, 1H), 7.38 (m, 2H), 7.45 (m, 2H) ppm. ^{13}C{^{1}H} NMR (C_6D_6): δ 5.63 (CH_3), 12.3 (CH_3), 12.7 (CH_3), 29.3 (CH), 62.0 (CH), 79.0 (CH_2), 119.8 (C), 120.3 (C), 124.9 (CH), 128.3 (CH), 128.5 (CH), 149.9 (C) ppm. Anal. Calcd for $C_{32}H_{48}SiTi$: C, 75.54; H, 9.53. Found: C,75.78; H, 9.51.

Cp*$_2$Ti(CHSiMe$_3$CHMeCH$_2$) (8). A glass bomb was charged with crystals of **2** (67.1 mg, 0.155 mmol) and 20 mL of C_6H_6. The solution was frozen (−195 °C) and degassed under vacuum. Propene (0.479 mmol) was condensed onto the frozen solution from a 138-mL bulb. The bomb was immersed in a 45 °C bath for 5 h, during which time the solution turned from green to red. The solution was then stirred at room temperature for 2 d. The volatile materials were removed under vacuum, and the resulting red powder was extracted into diethyl ether. The ether solution was reduced to 2 mL under vacuum and cooled to −50 °C to yield red crystals of **8** (54.5 mg, 78.8%). IR (cyclohexane): 3001(m), 2715 (w), 1994 (m), 1378 (s), 1243 (s), 1099 (s), 1072 (m), 1025 (m), 950 (m), 894 (m), 827 (s), 711 (s), 588 cm^{-1}. ^{1}H NMR (C_6D_6): δ 0.19 (m, 1H), 0.28 (s, 9H), 1.18 (d, ^3J = 6.0 Hz, 3H), 1.31 (m, 2H), 1.52 (m, 1H), 1.71 (s, 15H), 1.77 (s, 15H) ppm. ^{13}C{^{1}H} NMR (C_6D_6): δ 5.4 (CH_3), 12.2 (CH_3), 12.5 (CH_3), 14.4 (CH), 22.7 (CH_3), 75.0 (CH), 77.8 (CH_2), 118.7 (C), 118.9 (C) ppm. Anal. Calcd for $C_{27}H_{46}SiTi$: C, 72.59; H, 10.40. Found: C, 72.64; H, 10.64.

Cp*$_2$Ti(CHSiMe$_3$CHEtCH$_2$) (9). A glass bomb was charged with crystals of **2** (51.7 mg, 0.120 mmol) and 8 mL of C_6H_6. The solution was frozen (−195 °C) and degassed under vacuum. 1-Butene (0.362 mmol) was condensed onto the frozen solution from a 29.0-mL bulb. The bomb was immersed in a 45 °C bath for 3 h, during which time the solution turned from green to red. The solution was stirred an additional 12 h at 25 °C, and the volatile materials were removed under vacuum. The resulting red powder was extracted into diethyl ether and filtered. The volume of the filtrate was reduced to 1 mL under vacuum, and the solution was cooled to −50 °C for 12 h to yield red crystals of **9** (52.0 mg, 94.4%). IR (Nujol): 2721 (w), 1240 (s), 1099 (w), 1070 (w), 1018 (m), 929 (m), 898 (m), 848 (s), 825 (s), 744 (w), 715 (w), 665 (m) cm^{-1}. ^{1}H NMR (C_6D_6) δ −0.59 (m, 1H), 0.27 (s, 9H), 0.73 (m, 1H), 1.14 (m, 1H), 1.15 (t, ^3J = 7.26 Hz, 3H), 1.40 (d, ^3J = 13.1 Hz, 1H), 1.51 (m, 1H), 1.71 (s, 15H), 1.77 (s, 15H), 1.92 (m, 1H) ppm. ^{13}C{^{1}H} NMR (C_6D_6) δ 5.4 (CH_3), 12.2 (CH_3), 12.5 (CH_3), 13.9 (CH_3), 22.1 (CH), 30.5 (CH_2), 74.4 (CH), 74.9 (CH_2), 118.7 (C), 118.9 (C) ppm. Anal. Calcd for $C_{28}H_{48}SiTi$: C, 72.99; H, 10.52. Found: C, 72.72; H, 10.53.

Kinetic Study of Formation of 7 from 2 and Styrene. Stock solutions for runs performed at a constant styrene concentration were prepared as follows. An oven-dried 2-mL volumetric flask was charged with dimethoxybenzene (10.6 mg, 0.0771 mmol) and crystals of **2** (28.9 mg, 0.0668 mmol). A small amount of toluene-d_8 was added, followed by 250 μL (2.18 mmol) of styrene. The total volume was brought to 2 mL with toluene-d_8. The stock solution was stored at −50 °C until just prior to sample preparation. Samples were prepared by transferring 0.5 mL of the stock solution to an oven-dried J-Young NMR tube.

Stock solutions for runs performed with variable styrene concentrations were prepared as follows. An oven-dried 2-mL volumetric flask was charged with dimethoxybenzene (9.0 mg, 0.0651 mmol) and crystals of **2** (28.9 mg, 0.0668 mmol). The total volume was brought to 2 mL with toluene-d_8. The stock solution was stored at −50 °C until just prior to sample preparation. Samples were prepared by transferring 0.5 mL of the stock solution to an oven-dried J-Young NMR tube. The appropriate volume of styrene was added to each NMR tube using a gastight syringe. The solution for the kinetic study of the formation of **4** from **2** was prepared identically, except that no styrene was added.

The samples were lowered into the preheated probe of a Brucker AMX 300 spectrometer. The temperature in the probe was calibrated by measuring the peak separation of a sample of neat ethylene glycol.[70] Spectra were acquired periodically. To avoid any complications due to different relaxation times for the various resonances, spectra were recorded using one $\pi/2$ pulse. An automatic baseline correction was applied to the data. Integrals were placed manually but not phased. Absolute concentrations of each reagent were determined based on integration relative to the dimethoxybenzene resonance.

Kinetic Study of Formation of 4 and 7 from 2 in THF-d_8. The stock solution for runs performed in THF-d_8 was prepared as follows. An oven-dried 1-mL volumetric flask was charged with dimethoxybenzene (5.2 mg, 0.0376 mmol) and crystals of **2** (14.6 mg, 0.0337 mmol). The total volume was brought to 1 mL with THF-d_8. To an oven-dried J-Young NMR tube was transferred 0.5 mL of the stock solution, followed by 29 μL (0.253 mmol) of styrene. The remaining 0.5 mL of the stock solution was transferred to a second J-Young NMR tube and frozen (−78 °C) until just prior to the kinetic study of the formation of **4** from **2**, and the spectra were obtained as described above.

Reaction of 2 with Pyridine. Generation of 11. An NMR tube was charged with a solution of **2** (8.5 mg, 0.0197 mmol) in 0.5 mL of

(70) Amman, C.; Meier, P.; Merbach, A. E. *J. Magn. Reson.* **1982**, *46*, 319.

toluene-d_8. An initial ^{1}H NMR spectrum was recorded, and pyridine (16 μL, 0.198 mmol) was added via a syringe. The solution turned from green to reddish-orange upon addition of the pyridine. A ^{1}H NMR spectrum was recorded that showed a 55:45 mixture of **2** and **11**. ^{1}H NMR spectral data for **11**: δ 0.377 (s, 9H), 1.70 (s, 30H), 6.21 (s, 1H) ppm. The resonances for free and bound pyridine were coalesced, and gave broad peaks at δ 6.70, 6.99, and 8.47 ppm.

Reaction of 2 with DMAP. Generation of 12. An NMR tube was charged with a solution of **2** (4.6 mg, 0.011 mmol) in 0.3 mL of C_6D_6. DMAP was added to the tube as a solution in 0.2 mL of C_6D_6. The solution turned from green to purple upon addition of the DMAP. The ^{1}H NMR spectrum of the purple solution shows that it is a mixture of **2** and **12**. ^{1}H NMR spectral data for **12**: δ 0.534 (s, 9H), 1.93 (s, 30 H), 6.40 (s, 1H) ppm. The resonances for free and bound DMAP were coalesced, and gave broad peaks at δ 2.20, 6.10, and 8.46 ppm.

Cp*$_2$Ti(N$_2$C(H)(SiMe$_3$)CHCH) (14). A Schlenk flask was charged with **2** (200 mg, 0.462 mmol) in 10 mL of C_6H_6. Acetylene gas was bubbled through the solution for 10 min. The solution turned from dark green to red immediately, and the formation of polyacetylene was observed. The volatile materials were removed under vacuum, and the red oily residue was extracted into hexanes and cooled to −50 °C for 12 h to yield red crystals of **14** (116 mg, 54%). IR (Nujol): 1618 (w), 1606 (w), 1491 (m), 1448 (m), 1441 (m), 1433 (m), 1421 (m), 1414 (m), 1402 (m), 1298 (m), 1242 (m), 1227 (m), 1176 (m), 1132 (w), 1020 (m), 858 (m), 833 (m), 804 (m), 735 (m), 663 (w), 613 (m) cm^{-1}. ^{1}H NMR (C_6D_6): δ 7.29 (d, J = 9.4 Hz, 1H), 6.52 (d, J = 9.4 Hz, 1H), 6.33 (s, 1H), 1.74 (s, 30H), 0.36 (s, 9H) ppm. ^{13}C{^{1}H} (C_6D_6): δ 180.2 (CH), 133.3 (CH), 121.8 (C), 104.5 (CH), 12.4 (CH_3), −0.7 (CH_3) ppm. MS-EI m/z = 458 [M$^+$]. HRMS (EI) m/z calcd for $C_{26}H_{42}N_2SiTi$: calcd 458.2597, obsd 458.2589.

Cp*$_2$Ti(N(N=C(H)SiMe$_3$)C(Ph)CH) (17). Phenylacetylene (98.6 mg, 0.965 mmol) was added to a stirred solution of **2** (417.6 mg, 0.965 mmol) in C_6H_6 (10 mL). The solution turned red upon addition and was stirred for 15 min at 25 °C. The solution was concentrated to 5 mL and left at 25 °C for 5 d to yield red-black crystals of **17** (331 mg, 64%). IR (Nujol): 3062 (m), 3037 (m), 1591 (m), 1375 (s), 1323 (w), 1300 (w), 1265 (m), 1232 (s), 1171 (w), 1149 (w), 1097 (w) cm^{-1}. ^{1}H NMR (C_6D_6): δ 8.05 (d, 2 H), 7.34 (t, 2 H), 7.13 (t, 1 H), 6.34 (s, 1 H), 2.99 (s, 1 H), 1.68 (s, 30 H), 0.51 (s, 9 H) ppm. ^{13}C{^{1}H} NMR (C_6D_6): δ 192.3 (CH), 141.6 (C), 140.6 (C), 130.8 (CH), 128.1 (CH), 126.0 (CH), 125.5 (CH), 124.2 (C), 12.3 (CH_3), −0.96 (CH_3) ppm. MS-EI m/z = 534 [M$^+$]. Anal. Calcd for $C_{32}H_{46}N_2SiTi$: C, 71.88; H, 8.67; N, 5.24. Found: C, 71.73; H, 8.81; N, 5.06.

Cp*$_2$Ti(NN=CHSiMe$_3$)C(CH$_2$)CH$_2$ (18). A 50-mL glass bomb was charged with crystals of **2** (119 mg, 0.275 mmol) and 10 mL of toluene. The solution was frozen (−195 °C) and degassed under vacuum. Allene (0.275 mmol) was condensed onto the frozen solution from a 66-mL bulb. Upon warming to room temperature the solution turned from dark green to bright red, and the solution was stirred for 30 min. The volatile materials were removed under vacuum and the resulting red powder was extracted into hexanes. The volume of the hexanes solution was reduced to 3 mL under vacuum and cooled to −50 °C to yield red blocky crystals of **18** (98 mg, 77.8%). ^{1}H NMR (C_6D_6): δ 6.23 (s, 1H), 4.77 (d, J = 1.9 Hz, 1H), 3.78 (d, J = 1.9 Hz, 1H), 2.62 (s, 2H), 1.77 (s, 30H), 0.28 (s, 9H) ppm. ^{13}C{^{1}H} (C_6D_6): δ 138.4 (C), 137.6 (C), 124.3 (C), 72.8 (CH_2), 66.7 (CH_2), 12.3 (CH_3), −1.2 (CH_3) ppm. IR (Nujol): 1902 (w), 1576 (m), 1566 (w), 1512 (m), 1502 (m), 1493 (m), 1481 (m), 1466 (m), 1460 (m), 1456 (m), 1441 (m), 1425 (m), 1412 (m), 1402 (w), 1371 (m), 1348 (w), 1290 (m), 12464 (m), 1107 (m), 1022 (w), 1003 (w), 887 (m), 864 (m), 841 (m), 825 (m), 806 (m), 744 (m), 727 (m), 688 (w), 667 (w), 617 (m) cm^{-1}; MS-EI m/z = 472 [M$^+$]. Anal. Calcd for $C_{27}H_{44}N_2SiTi$: C, 68.61; H, 9.38; N, 5.93. Found: C, 68.79; H, 9.54; N, 5.62.

Cp*$_2$Ti(N(H)N=C(SiMe$_3$)O) (19). A 60-mL glass bomb was charged with crystals of **2** (116 mg, 0.267 mmol) and 10 mL of C_6H_6. The solution was frozen (−195 °C) and degassed under vacuum. N_2O (0.267 mmol) was condensed onto the frozen solution from a 66-mL bulb. Upon warming to room temperature the solution turned from dark green to dark red, and the solution was stirred for 40 min. The volatile materials were removed under vacuum and the resulting red powder was extracted into ether. The ether solution was reduced to 8 mL under vacuum and cooled to −50 °C to yield red microcrystals of **19** (48 mg, 54.0%). ^{1}H NMR (C_6D_6): δ 8.09 (br, 1H), 1.74 (s, 30H), 0.46 (s, 9H) ppm. ^{13}C{^{1}H} (C_6D_6): δ 177.1 (C), 122.1 (C), 11.7 (CH_3), −0.4 (CH_3) ppm. IR (Nujol): 3290 (w), 2214 (m), 2197 (m), 1959 (w), 1954 (w), 1948 (w), 1938 (w), 1917 (m), 1902 (m), 1514 (w), 1414 (w), 1402 (w), 1371 (m), 1321 (w), 1277 (m), 1244 (m), 1176 (w), 1163 (w), 1020 (m), 991 (w), 976 (w), 953 (w), 914 (m), 841 (m), 808 (w), 752 (m), 723 (w), 692 (w), 656 (w), 631 (m) cm^{-1}; MS-EI m/z = 448 [M$^+$]. Anal. Calcd for $C_{24}H_{40}N_2OSiTi$: C, 64.26; H, 8.99; N, 6.24. Found: C 64.10; H, 9.20; N, 5.86.

X-ray Crystallographic Study of Cp*$_2$Ti(N$_2$CHSiMe$_3$) (2). Crystals of **2** suitable for X-ray diffraction were obtained by slow cooling of a hexanes solution of **2** to −50 °C. A fragment of one of these green blocky crystals having dimensions of 0.20 × 0.23 × 0.28 mm was mounted on a glass fiber using Paratone N hydrocarbon oil. All measurements were made on a Siemens SMART (Siemens Industrial Automation, Inc.) diffractometer with a CCD area detector using graphite monochromated Mo Kα radiation. All calculations were performed using the TEXSAN crystallographic software package of Molecular Structure Corporation.

Cell constants and an orientation matrix obtained from a least-squares refinement using the measured positions of 7153 reflections in the range $3.00 < 2\theta < 45.00°$ corresponded to a primitive monoclinic cell with dimensions given as Supporting Information. The final cell parameters and specific data collection parameters for this data set are given in Table 1 or as Supporting Information. The systematic absences of $h0l$: $h + l \neq 2n$ and $0k0$: $k \neq 2n$ uniquely determined the space group to be $P2_1/n$ (#14).

Data were integrated to a maximum 2θ value of 46.5 ° using the program SAINT with box parameters of 1.6 × 1.6 × 0.6°. The data were corrected for Lorentz and polarization effects. No decay or absorption correction was applied. The 9838 integrated reflections were averaged to 3629 unique data (including systematic absences) (R_{int} = 0.068). The structure was solved by direct methods and expanded using Fourier techniques. All non-hydrogen atoms were refined anisotropically, and hydrogen atoms were refined with isotropic thermal parameters. A correction for secondary extinction was applied to the data in the last cycles of least-squares (coefficient = 1.27765 × 10^{-6}). One datum was removed from the least-squares refinement due to evidence of multiple diffraction. The final cycle of full-matrix least-squares refinement was based on 2904 observed reflections ($I > 3.00\sigma(I)$) and 414 variable parameters and converged (largest parameter shift was 0.01 times its esd) with unweighted and weighted agreement factors of R = 0.045 and R_w = 0.058. The standard deviation of an observation of unit weight was 2.23. The weighting scheme was based on counting statistics and included a factor (p = 0.030) to downweight the intense reflections. The maximum and minimum peaks on the final difference Fourier map corresponded to 0.28 and −0.33 e$^-$/Å^3 respectively. Selected bond lengths and angles are given in Table 2, and an ORTEP is shown in Figure 1. Positional and anisotropic thermal parameters, tables of bond lengths and angles, and complete crystal and data collection parameters are provided as Supporting Information.

X-ray Crystal Structure of Cp*$_2$Ti(CH(SiMe$_3$)CH(Me)CH$_2$) (8). Red rodlike crystals of **8** suitable for X-ray diffraction were grown by slow cooling of an ether solution of **8** to −50 °C. The crystal mounting and data collection were performed as described for the X-ray crystallographic analysis of **2**. The specific data collection parameters are given in Table 1 or as Supporting Information. Non-hydrogen atoms were refined anisotropically. The hydrogen atom coordinates were refined but their isotropic B's were fixed. Selected bond lengths and angles are given in Table 3, and an ORTEP is shown in Figure 3. Positional and anisotropic thermal parameters, tables of bond lengths and angles, and complete crystal and data collection parameters are provided as Supporting Information.

X-ray Crystal Structure of Cp*$_2$Ti(N(N=C(H)SiMe$_3$)C(CH$_2$)CH$_2$) (18). Crystals of **18** suitable for X-ray diffraction were obtained by slow cooling of a hexanes solution of **18** to −50 °C. A red triangular-shaped crystal having dimensions of 0.35 × 0.35 × 0.16 mm was mounted on a glass fiber using Paratone N hydrocarbon oil. All measurements were made on a Siemens SMART (Siemens Industrial Automation, Inc.) diffractometer with a CCD area detector using

graphite monochromated Mo Kα radiation. All calculations were performed using the TEXSAN crystallographic software package of Molecular Structure Corporation.

Cell constants and an orientation matrix obtained from a least-squares refinement using the measured positions of 5538 reflections in the range $3.00 < 2\theta < 45.00°$ corresponded to a primitive triclinic cell with dimensions given as Supporting Information. The final cell parameters and specific data collection parameters for this data set are given in Table 1 or as Supporting Information. On the basis of a statistical analysis of intensity distribution, and the successful solution and refinement of the structure, the space group was determined to be $P\bar{1}$ (#2).

Data were integrated to a maximum 2θ value of 51.9 ° using the program SAINT with box parameters of 1.6 × 1.6 × 0.6°. The data were corrected for Lorentz and polarization effects. No decay correction was applied. An empirical absorption correction based on comparison of redundant and equivalent data and an ellipsoidal model of the absorption surface was applied using the program XPREP (Siemens Industrial Automation, Inc.) where $T_{max} = 0.91$ and $T_{min} = 0.88$. The 7493 integrated and corrected reflections were averaged to 4601 unique data ($R_{int} = 0.025$). The structure was solved by direct methods and expanded using Fourier techniques. All non-hydrogen atoms were refined anisotropically, and hydrogen atoms were included but not refined. The final cycle of full-matrix least-squares refinement was based on 3941 observed reflections ($I > 3.00\sigma(I)$) and 280 variable parameters and converged (largest parameter shift was 0.01 times its esd) with unweighted and weighted agreement factors of $R = 0.039$ and $R_w = 0.057$. The standard deviation of an observation of unit weight was 2.15. The weighting scheme was based on counting statistics and included a factor ($p = 0.030$) to downweight the intense reflections. The maximum and minimum peaks on the final difference Fourier map corresponded to 0.26 and −0.32 e−/Å^3 respectively. Selected bond lengths and angles are given in Table 4, and an ORTEP is shown in Figure 7. Positional and anisotropic thermal parameters, tables of bond lengths and angles, and complete crystal and data collection parameters are provided as Supporting Information.

Acknowledgment. We thank the National Institutes of Health (Grant No. GM-25459) and the Arthur C. Cope Fund administered by the American Chemical Society for generous financial support of this work. We thank Dr. F. J. Hollander, director of the University of California Berkeley College of Chemistry X-ray diffraction facility (CHEXRAY), and Dr. P. Goodson for solving the crystal structures of **2**, **8**, and **18**. This paper is dedicated to Professor Warren T. Roper, for his many ground-breaking contributions to organometallic chemistry, on the occasion of his 60th birthday.

Supporting Information Available: Tables of positional and thermal parameters and intramolecular bond lengths and angles for the structures of **2**, **8** and **18**, NOESY spectrum of **9** (21 pages, print/PDF). See any current masthead page for ordering information and Web access instructions.

JA974303D